Canadian Journal of Fisheries and Aquatic Sciences

Article

The influence of age and cohort on the distribution of walleye pollock (*Gadus chalcogrammus*) in the eastern Bering Sea

Duane E. Stevenson[a], **Stan Kotwicki**[a], **James T. Thorson**[a], **Giancarlo M. Correa**[b], **and Troy Buckley**[a]

[a]National Marine Fisheries Service, Alaska Fisheries Science Center, 7600 Sand Point Way NE, Seattle, WA 98115, USA; [b]Oregon State University, College of Earth, Ocean, and Atmosphere Sciences, Corvallis, OR 97330, USA

Corresponding author: **Duane E. Stevenson** (email: duane.stevenson@noaa.gov)

Abstract

The spatial distributions of marine fish populations are influenced by environmental conditions, intrinsic properties of the populations, and prior distribution. The influence of these factors may not be consistent across age classes. For this study, age composition estimates for walleye pollock (*Gadus chalcogrammus*) collected on bottom-trawl surveys in the Bering Sea were used to estimate range correlation indices, population centers of gravity, and effective area occupied. Age-specific density maps suggested a circular ontogenic migration during the summer feeding season, with the youngest and oldest groups most broadly distributed. Range correlation analysis among age groups and year classes provided clear evidence of a population cohort effect in the spatial distribution of the population. Variance decomposition analysis indicated that the variance in the spatial distribution of age groups during summer was influenced by the initial distribution of that cohort as recruits. Model-based analyses showed that extrinsic temperature variables affected the youngest and oldest age classes the most, but provided no indication of age-related effects for intrinsic population factors. This study showed that both cohort and age-specific factors are important drivers of spatial distribution.

Key words: demographics, age composition, distribution, walleye pollock, modeling, VAST

Résumé

La répartition spatiale de populations de poissons marins est influencée par les conditions ambiantes, des propriétés intrinsèques des populations et la répartition préalable. L'influence de ces facteurs pourrait ne pas être uniforme d'une classe d'âge à l'autre. Nous avons utilisé des estimations de la composition par âge pour des goberges de l'Alaska (*Gadus chalcogrammus*) prélevées dans le cadre d'évaluations au chalut de fond dans la mer de Behring pour estimer des indices de corrélation des aires de répartition, les centres de gravité de la population et la superficie occupée effective. Des cartes de densité selon l'âge indiqueraient une migration ontogénétique circulaire durant la saison d'alimentation estivale, les groupes les plus jeunes et les plus vieux présentant les répartitions les plus vastes. L'analyse de corrélation des aires de répartition de différents groupes d'âge et classes d'année fournit des preuves claires d'un effet populationnel de la cohorte dans la répartition spatiale de la population. L'analyse de décomposition de la variance indique que la variance de la répartition spatiale des groupes d'âge durant l'été est influencée par la répartition initiale de la cohorte au moment du recrutement. Des analyses reposant sur des modèles montrent que des variables extrinsèques associées à la température exercent la plus grande influence sur les classes d'âge les plus jeunes et les plus vieilles, mais elles ne révèlent aucun effet relié à l'âge de facteurs intrinsèques à la population. L'étude démontre que des facteurs associés tant à la cohorte qu'à l'âge exercent une importante influence sur la répartition spatiale. [Traduit par la Rédaction]

Mots-clés : démographie, composition par âge, répartition, goberge de l'Alaska, modélisation, VAST

Introduction

The spatial distributions of fish populations are influenced by many factors. Environmental variables that define habitat suitability are clearly important. For example, physiological tolerances and resource availability directly affect the ability of a species to survive in a particular habitat. These factors have historically been used to define the fundamental and realized niche of a species, in the sense originally defined by Hutchinson (1957). However, other factors intrinsic to the population profoundly affect how a species occupies its realized niche. Recruitment dynamics, age structure, site fidelity, and behavioral preferences are some of the many

intrinsic factors that may affect the spatial distribution of a population. Planque et al. (2011) listed two categories of extrinsic drivers of spatial distribution (geographic attachment and environmental conditions), and four categories of intrinsic drivers (density-dependent habitat selection, spatial dependency, demographic structure, and species interactions). They also listed a third type of driver (spatial memory), which is a product of the current and past distribution of the population and represents an extension of the entrainment hypothesis developed by Petitgas et al. (2006) and MacCall et al. (2019).

Because the distribution of a population can be influenced by both extrinsic environmental and intrinsic population factors, and is also dependent on past distribution, modeling efforts seeking to describe and predict the spatial distribution of a population may be improved by including both types of factors as well as a "memory" component. Models incorporating a combination of extrinsic and intrinsic factors can be used to assess the relative impacts of these factors using a variance decomposition process, in which variance in the spatial distribution of the population is decomposed into extrinsic and intrinsic effects to assess which effects are dominant. This "variance decomposition" approach avoids an artificial accept–reject outcome that results from hypothesis testing (Thorson and Minto 2015) and is appropriate in a world of multicausality and tapering effects (Burnham and Anderson 2002). The relative effects of spatial memory on the distribution of a population can also be assessed through spatial comparisons of temporally distinct components of the population, such as recruitment classes (cohorts).

In addition to assessing the relative importance of intrinsic and extrinsic factors on the spatial distribution of a population, it may be desirable to know how these factors affect different segments of that population. While the bulk of studies in spatial ecology have focused on population centroids (Pinsky et al. 2013) or range edges (Fredston-Hermann et al. 2020), there has been comparatively little investigation of mechanisms defining shifts in the spatial distribution in age-specific (or size-specific) segments of fish populations (but see Marquez et al. 2021). For species targeted by commercial fisheries, the distribution of desirable age (or size) classes and the factors that drive the spatial distributions of those population segments are of particular interest.

The walleye pollock (*Gadus chalcogrammus*; hereinafter pollock) population of the eastern Bering Sea (EBS) supports one of the most valuable fisheries in the world, with approximately 1 million metric tons harvested commercially each year for the past 50 years (Ianelli et al. 2019). Although pollock biomass estimates have remained relatively stable in recent years, there is a growing body of evidence that the Bering Sea ecosystem is changing. The formation of seasonal sea ice that once acted as the prime driver of ecosystem functions in the Bering Sea has been declining as the water temperatures in the region have warmed (Stabeno et al. 2017). As the water warms, there is evidence that the pollock population of the EBS is moving north into the Arctic (Stevenson and Lauth 2019) and west past the US–Russia convention line (O'Leary et al. 2021).

The distribution and movements of pollock in the EBS have been studied in a number of contexts. Spawning occurs in two major pulses, with the first in February–March largely centering in the southeastern Bering Sea near Bogoslof and Unimak Islands, and the second in April–May farther north, near the Pribilof Islands (Hinckley 1987; Kim et al. 1996; Bacheler et al. 2010). The distribution of juvenile pollock has been studied in relation to many factors, including the warm and cold stanzas that have dominated the EBS over the past 20 years (Duffy-Anderson et al. 2017), resulting in overlap between juvenile pollock and predators/competitors (Thorson et al. 2021) and small-scale habitat heterogeneity (Benoit-Bird et al. 2013). Kotwicki et al. (2005) described seasonal feeding migrations in pollock, noting that as the water warms in the spring and summer, adult pollock migrate northwestward and onshore from their spawning grounds in the EBS. Their results also suggested that juvenile pollock complete similar annual migrations, but cover shorter distances. Ianelli (2005) briefly described ontogenic migration, with younger fish more common on the northwestern part of the EBS shelf and older fish moving progressively to the south and east of the EBS shelf.

The pollock is considered a semi-pelagic species, and the vertical distribution of pollock in the water column is complex. Early life stages are generally found near the surface (Smart et al. 2013; Parker-Stetter et al. 2015),but after the first year, they transition to midwater and demersal habitats. Midwater acoustic surveys and bottom-trawl surveys in Alaska suggest that age-1 pollock tend to school close to the bottom, while age-2 and other juvenile pollock stay higher in the water column, and adults are primarily demersal (Duffy-Anderson 2003; Honkalehto et al. 2010; Kotwicki et al. 2015; Lauth et al. 2019). The proportion of the population available to the bottom trawl varies spatially, over time, and by age, although over 50% is available to the bottom trawl in any year previously documented (Monnahan et al. 2021).

In this study, we seek to test three main questions about the distribution of pollock in the EBS:

1. Is there evidence of a memory/entrainment effect in the relative distributions of cohorts (recruitment classes) in the population?
2. What are the relative influences of environmental conditions (year effects) and memory/entrainment (cohort effects) on the population center of distribution?
3. Do intrinsic and extrinsic factors affecting the effective area occupied (EAO) by the population differ among age classes?

We explore these questions using a combination of analyses that include model-based predictions of density for age-specific segments of the pollock population of the EBS from 1982 through 2019. In addition, a variance decomposition procedure was used to assess the relative importance of survey year and cohort to the variance in spatial distribution among age-cohort combinations. The primary goal of these investigations was to evaluate the relative contributions of survey year (year of collection) and cohort (year of birth) to the spatial distributions of age-specific segments of the

pollock population. The primary importance of this study is that it assesses the relative magnitude of intrinsic, extrinsic, and cohort effects influencing the spatial distribution of different age segments of a marine fish population.

Materials and methods

Data collection and age composition estimates

Data used in this study were collected during bottom trawl surveys of the EBS shelf, conducted annually by the Alaska Fisheries Science Center (AFSC) of the U.S. National Marine Fisheries Service from 1982 through 2019 (e.g., Lauth et al. 2019). These fixed-station surveys used an otter trawl with an effective fishing height of approximately 16 m for pollock (Kotwicki et al. 2015). Thus, the spatial trends analyzed here apply only to the demersal portion of the population available to the trawl. The survey grid consists of 376 stations, each of which is sampled annually. At each station, random subsamples of length-frequency data were collected (totaling roughly 20 000–50 000 lengths per year), as well as otoliths (totaling roughly 1000–2000 otoliths per year) from either length-stratified (2006 and prior) or random (2007–2019) subsamples of the total catch. Age data were then combined with length abundance information to obtain age-specific abundances at each station using a model-based approach. This approach consisted of using continuation ratio logits to model the probability of being a specific age at a given length, taking into account the spatial variability in size-at-age (Berg and Kristensen 2012; Correa et al. 2020). Techniques used at the AFSC to age pollock have been radiometrically validated up to age-8 (Kastelle and Kimura 2006); therefore, all specimens with estimated ages higher than 8 years (approximately 25% of all aged specimens) were combined into the "age-9+" class.

A dataset including density-at-age estimates for each age class, for each survey station, for each survey year was used to create a multispecies spatiotemporal model in VAST (vector-autoregressive spatiotemporal modeling package; Thorson and Barnett 2017), version 3.4.0, in which age classes were treated as separate species in a multivariate model. VAST uses template model builder to identify maximum likelihood estimates (Kristensen et al. 2016), the stochastic partial differential equation (SPDE) method to rapidly approximate spatial correlations (Lindgren et al. 2011), and a generalization of the delta-method to calculate standard errors for parameters and derived quantities (Tierney et al. 1989). We specified gamma-distributed positive catch rates and the alternative "Poisson-linked" delta model using a log-link function for encounter probabilities. The region specified was "eastern_bering_sea", corresponding to the spatial footprint of the annual bottom trawl survey operated by AFSC in the EBS. The spatial resolution was set at 500 knots, representing a relatively fine-scale mesh for density predictions that are still computationally feasible, and corresponds roughly with the spatial resolution of the samples (376 stations). We included both spatial and spatiotemporal components as well as an annual intercept for each of two linear predictors, and did not estimate any temporal autocorrelation in either intercepts or spatiotemporal components. By avoiding any temporal autocorrelation, we ensured that resulting density predictions are "exchangeable" for each of the ages and year-within-age. This, in turn, justifies our statistical analysis of density patterns for each age and year, which we treat as independent for each age–year combination in the analyses.

Outputs used from the VAST model included rasters (with the grid cell size of approximately 100 km^2) of pollock density estimates by age (Supplementary material A), center of gravity location, and estimates of EAO by age (Thorson et al. 2016). Cumulative density plots for each age class were created by calculating the average estimated density across all years for each of the 5000 grid cells from the VAST output raster, then sorting grid cells in order of descending density and plotting the cells required to reach 75% of the cumulative average density. The 75% threshold for cumulative density was chosen to visualize contrasts between spatial distributions of age classes and to align with the regional definition of "principal Essential Fish Habitat area" (see Laman et al. 2018, their figure 8). Centers of gravity were obtained for each age class for each year using biomass-weighted eastings and northings in Universal Transverse Mercator (UTM) coordinates (see Thorson 2019, their table 2). Mean centers of gravity for each age class were calculated as the simple average of the latitude and longitude of the centers of gravity for each survey year. Longitude and latitude anomalies for each age–year combination were obtained by subtracting the mean longitude/latitude (in UTM coordinates) from the mean of the 38 longitude/latitude estimates for that age class. Temporal trends in center of gravity (COG) were depicted by plotting these anomalies for all age classes over the study period (1982–2019). VAST generates estimates of EAO for each age–year combination (see Thorson 2019, their table 2), which are calculated as the area required to contain the population at its biomass-weighted average density (Thorson et al. 2016).

Question 1: evidence of a cohort effect

If the spatial distribution of pollock is being driven by contemporary factors, either intrinsic or extrinsic, operating simultaneously on the entire population, then we expect correlations among the distributions of all age classes within each year to be greater than correlations among different survey years. However, if there is a memory effect operating on different cohorts to influence the spatial distribution of pollock, then we expect correlations within cohorts (as they are repeatedly sampled in successive survey years) to be greater than those among different cohorts. We therefore used two metrics of range correlation, the global index of collocation (GIC) and Schoener's D, to investigate spatial correlations among the distributions of pollock age groups. GIC uses pairwise comparisons of population centers of gravity as an indicator of large-scale similarity among distributions (Bez and Rivoirard 2000; Woillez et al. 2009; Kotwicki and Lauth 2013), while Schoener's D (Schoener 1968) uses station-by-station pairwise comparisons to assess fine-scale spatial similarity among distributions. We use both metrics, given that fine-scale overlap (measured by Schoener's D) will capture high-resolution processes while regional overlap (measured by GIC) will capture low-resolution processes.

Metrics of range correlation were calculated from the grid cell density predictions of the VAST model (5000 grid cells). GIC values were calculated in R using the method of Kotwicki and Lauth (2013):

$$\text{GIC}_{1,2} = 1 - \frac{\Delta\text{COG}_{1,2}{}^2}{\Delta\text{COG}_{1,2}{}^2 + I_1 + I_2} \quad (1)$$

where ΔCOG is the distance between COGs for a given pair of age–year groups, I_1 is the dispersion for group 1 and I_2 is the dispersion for group 2. The dispersion for each group is calculated as

$$I_1 = \frac{\sum_{i=1}^{n} (\Delta\text{COG}_{1,2})^2 z_{1i}}{\sum_{i=1}^{n} z_{1i}} \quad (2)$$

Schoener's *D* values were calculated in R using the Species Association Analysis (spaa) package, version 0.2.1 (Zhang 2016):

$$D = 1 - 0.5 \times \sum_{i=1}^{n} |p_{x,i} - p_{y,i}| \quad (3)$$

where $p_{x,i}$ and $p_{y,i}$ are the proportions of age–year x and y, respectively, at station i.

For each range correlation metric, GIC, and Schoener's *D*, a matrix of pairwise correlation statistics was generated for each age–year combination (9 ages × 38 data years = 342 × 342 matrix). A one-tailed *t* test was then performed to determine whether the mean of within-year correlations for each age pairing (e.g., age-1 vs. age-2 from 1982, $n = 38$) was significantly higher than the mean of all possible age class correlations (e.g., age-1 from 1982 vs. age-2 from 1985, $n = 741$). Significant results for these *t* tests were interpreted to indicate significant spatial correlations between age classes within years. The same analysis was repeated for age–cohort combinations (e.g., age-2 specimens collected in 1985 would represent the 1983 cohort, also a 342 × 342 matrix), and significant results were interpreted to indicate significant spatial correlations between age classes within cohorts.

Question 2: relative importance of effects for center of gravity

The relative importance of survey year and cohort to the variance explained in the linear model predicting latitude/longitude of the COG estimates by age was assessed using a variance decomposition procedure described in the R package *relaimpo*, which uses statistical metrics to evaluate the relative importance of the regressors (Grömping 2006). Relative importance was estimated using the following models:

$$\text{lm1} : \text{lm}(\text{Ndev} \sim \text{factor}(\text{Year}) + \text{factor}(\text{Cohort}))$$
$$\text{lm2} : \text{lm}(\text{Edev} \sim \text{factor}(\text{Year}) + \text{factor}(\text{Cohort}))$$

where Ndev and Edev are northing and easting deviations from the mean COG for a given age class, and Year and Cohort are factors predicting distribution. The effect of Year was used to capture all known and unknown year-specific effects that influence pollock distribution, including temperature (Kotwicki et al. 2005; Thorson et al. 2017; Eisner et al. 2021), light conditions (Kotwicki et al. 2015), fish density, fishing pressure, ecological teleconnections resulting from regional warm/cool conditions (Thorson et al. 2021), etc. The effect of Cohort is used to capture all cohort-specific effects that influence pollock distribution, including specifics of cohort origination, cohort survival, multiyear effects on cohort distribution, differences in ontogenetic migrations between cohorts, and other cohort related variables. Quantification of an individual regressor's contribution to these regression models was estimated using three metric outputs from the function *calc.relimp* in the R package *relaimpo* (Grömping 2006). The metric "first" represents variance explained by each predictor alone; the metric "last" in this case represents additional variance explained by each predictor when added to the model after the variance explained by the first variable is accounted for; and the metric "lmg" is the average contribution to variance explained for both orders of predictors (Christensen 1992; Grömping 2006).

Question 3: age-related factors influencing effective area occupied

Finally, we seek to identify which intrinsic/extrinsic/memory effects are associated with larger or smaller EAO for each combination of age and year. To do so, we used a generalized additive modeling (GAM) procedure to assess the effects of some population parameters and environmental variables, including age-1 abundance, spawning stock biomass, mean surface temperature, cold pool area, and age class, on EAO. These models were constructed in R using the "gam" function of the mgcv package, version 1.8-31 (Wood 2017). Age-1 abundance and spawning stock biomass were obtained from the 2019 assessment of the pollock stock in the EBS (Ianelli et al. 2019, their table 32). Water temperatures were recorded by a bathythermograph placed on the headrope of the net; surface temperature was recorded at 1 m depth, and bottom temperature was recorded while the net was on bottom in fishing configuration, ~3 m off bottom. Mean annual surface temperatures were calculated as the average of water temperature samples from each survey station sampled by AFSC's EBS bottom trawl survey, weighted by the proportion of their assigned stratum area. Four different near-bottom temperature variables were tested in GAMs, including annual average bottom temperature, calculated in the same way as surface temperature, and three different cold pool area variables, calculated as in Kotwicki and Lauth (2013) for three different temperatures (0, 1, and 2 °C). EAO estimates were weighted by $1/\text{SE}^2$ in the model to correct for uncertainty, where SE is the estimated standard error generated by VAST, and weighting by precision accounts for heteroscedasticity when fitting the GAM model.

The initial model investigated was

$$\text{EAO} \sim \text{factor}(\text{age}) + s(\text{cpa}, k = 4) + s(\text{stemp}, k = 4) + s(\text{ssb}, k = 4) + s(\text{rec}, k = 4)$$

where EAO is the effective area occupied (from VAST model, weighted by $1/\text{SE}^2$), age is the age class, cpa is the cold pool

area (the near-bottom temperature variable), stemp is the mean annual surface temperature, ssb is the standing stock biomass, and rec isage-1 abundance. Smooth effects were restricted to a maximum of four knots to minimize the possibility of overfitting. First, the best of the four cold pool covariates (annual bottom temperature, or cold pool area less than 0, 1, or 2 °C) was chosen by comparing four potential versions of the initial model above, using Akaike Information Criterion (AIC). The model with the lowest AIC was used as the initial model for testing for differences between the smooth effects by age, using "by" argument (e.g., *s*(cpa, by = factor(age), $k = 4$)). This age factor was added to initial model smooth covariates one by one and tested for model improvements using AIC. The "by" parameter was retained in the covariate for which the AIC was reduced the most. The process was repeated until no more reduction in AIC could be achieved or until all variables included the "by" argument.

Results

Describing age-specific densities

The results of the VAST model show distinct differences in the spatial distribution of age classes of pollock in the EBS. Predicted density plots for all survey years combined (Fig. 1) show that the youngest pollock (age-1) are on average broadly distributed across the shelf to the north of the Pribilof Islands from the inner domain to the shelf edge. Age-1 and age-2 pollock are rarely encountered south of the Pribilof Islands. Progressing through the juvenile stage (ages 2 and 3), pollock are more concentrated near the shelf edge, becoming largely absent from the inner shelf and remaining most densely distributed to the north of the Pribilof Islands. Young adult pollock (age-4 through age-7) remain concentrated on the outer shelf, with their distribution moving slightly to the south and west with each successive age class. For the oldest age classes examined in this study (age-8 and age-9+), the distribution spreads back onto the middle shelf, and high densities of pollock are increasingly found in the southern Bering Sea near the Alaska Peninsula.

Mean COG calculated for each age class over the survey period summarizes the distribution trends indicated in the density plots. These age-specific COGs describe a u-shaped or nearly circular trend in centers of distribution as pollock age (Fig. 2). The transition from age-1 to age-2 is marked by a notable northwestward shift in distribution, reflecting the increasing concentration of individuals near the shelf edge in the northern part of the survey area. All subsequent age transitions generally reflect a southward and eastward movement of the older segments of the population. Transitions from age-3 through age-8 indicate only minor shifts in distribution, and although the movement is directionally consistent, it appears gradual. The transition from age-8 to the oldest age class (age-9+) appears more significant. The COG for this oldest age group is shifted notably to the east, reflecting the spread of this population segment back onto the middle shelf as well as the increasing proportion of the population in the southeastern portion of the Bering Sea.

In addition to differences in their population COG, pollock occupy varying amounts of space as they age. Mean estimates of EAO over the survey period indicate that age-1 pollock are highly dispersed, occupying much more EAO than subsequent year classes (Fig. 3). Older juveniles (age-2 through age-4) are much more concentrated, occupying on average less than half the area of age-1 fish. Adult pollock (age-5 through age-9+) are progressively more dispersed, with the oldest age classes occupying the largest area. These trends are also visible in the density plots (Fig. 1).

Our data also show evidence of some temporal trends in pollock distribution. For example, over the 38-year study period, the COG averaged over all age classes of pollock moved significantly northward (Fig. 4), although longitude did not shift significantly. Furthermore, the average EAO has increased substantially, particularly over the last decade.

Question 1: evidence of a cohort effect

Measures of spatial correlation based on range overlap metrics indicate strong correlations among age groups both within year and within cohort. Within year, GIC values were significantly correlated (Table 1) for all adjacent age groups (e.g., age-2 vs. age-3, age-3 vs. age-4) as well as a few age groups separated by two years (e.g., age-4 vs. age-6). None of the more distant age groups (three or more age classes apart) were significantly correlated. Schoener's *D* values (Table 2) within year were significantly correlated for nearly all pairwise comparisons, regardless of age class, although age-1 and age-9+ comparisons were less universally significant. Many of the pairwise comparisons of spatial correlation within cohort were also significant. GIC values (Table 1) were significantly correlated among the majority of adjacent age groups, as well as several nonadjacent age groups (e.g., age-3 vs. age-6). Schoener's *D* values (Table 2) demonstrated a similar pattern, with nearly all adjacent comparisons significant, as well as many of the nonadjacent comparisons.

Thus, the spatial distributions of pollock age classes were generally highly correlated within a survey year, particularly those of the adjacent age classes. This effect was more pronounced when measured using the finer scale Schoener's *D* statistic. Correlation patterns within a cohort were generally similar, indicating that the spatial distributions of individual cohorts are highly correlated as they progress through time, again particularly across a single age step. Significant pairwise correlations within a year indicate that the spatial distribution of age classes within the population is being driven by extrinsic or intrinsic factors operating simultaneously on the whole population, while the significant pairwise correlations within a cohort for the majority of cohorts indicate that the spatial distribution of those cohorts is, to some extent, driven by spatial memory or entrainment. For example, the distribution of age-3 pollock in 1990 was significantly influenced by the distribution of age-2 pollock in 1989.

Question 2: centers of gravity

The linear models in which age-specific COG (decomposed into deviations from the mean latitude and longitude) are related to the factor variables "Year" and "Cohort" extend and

Fig. 1. Plots of 75% cumulative estimated density (latitude/longitude projected in NAD83), averaged over the survey period (1982–2019), for age classes of pollock. Plus signs (+) indicate the mean center of gravity for each age class, averaged over the survey period. [Colour online.]

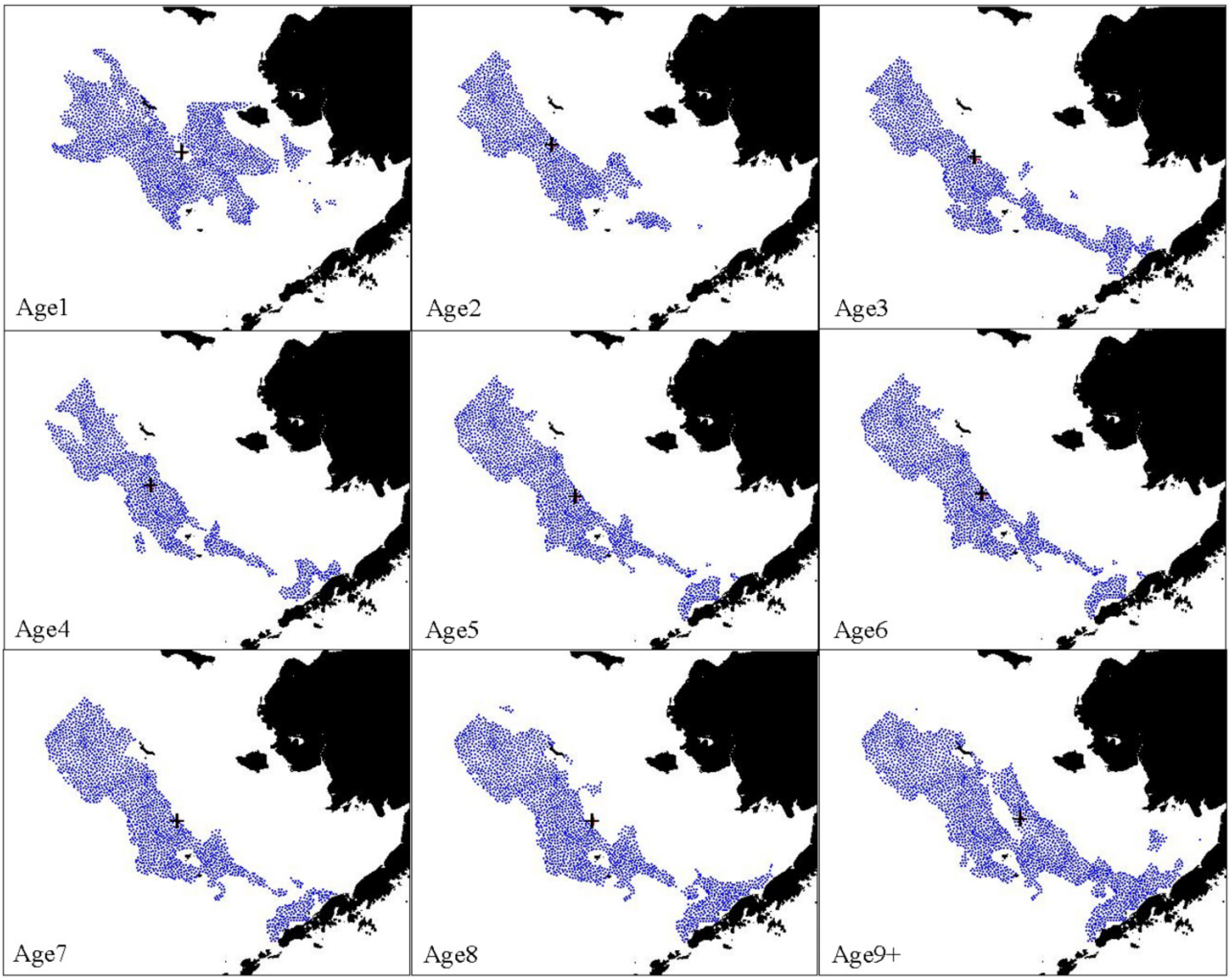

clarify the results of the range correlation metrics. In both the latitude and longitude models, year and cohort contribute significantly to the overall variance of the model (Table 3) and explain the majority of variation in the data (>60%). Furthermore, the relative contributions of the two factors are similar in both models, with year contributing approximately two-thirds of the variance, and cohort contributing approximately one-third. These results indicate that both year and cohort contribute significantly to variation in both the latitudinal and longitudinal axes of spatial variation in the distribution of pollock, though the magnitude of the year effect is clearly greater.

Question 3: effective area occupied

The results of the GAM modeling of EAO are presented in Tables 4 and 5. Of the near-bottom temperature variables tested (cold pool area <0, <1, <2 °C, or mean annual bottom temp), the cold pool area <0 °C resulted in the lowest AIC. Differences in the smooth effect by age were detected only for the environmental variables "cpa" and "stemp" (Table 4). Thus, in the final model:

$$\begin{aligned}\text{EAO} \sim \text{factor}(\text{age}) &+ s(\text{cpa}, \text{by} = \text{factor}(\text{age}), k = 4)\\ &+ s(\text{stemp}, \text{by} = \text{factor}(\text{age}), k = 4)\\ &+ s(\text{ssb}, k = 4) + s(\text{rec}, k = 4)\end{aligned}$$

The final model explained a large proportion of the observed variation in EAO (80.6%). The relationship between age and EAO reflected the same trend as above (Fig. 3), with the youngest and oldest age classes occupying the most space, and the older juveniles (age-2 through age-4) being the most concentrated (Fig. 5A). The age factor alone explained 61.4% of the variation in EAO. For the population variables biomass (ssb) and age-1 abundance (rec), we did not detect differences between smooth terms by age, but the results indicated that lower values of these variables result in lower EAO (Figs. 5B and 5C). For biomass, results suggest that the EAO is smaller than average for ssb values lower than 2500 (=2.5 million tons). For recruitment, results indicate that EAO is more extensive than average only for the six largest cohorts (based on age-1 abundance).

Fig. 2. Estimated centers of gravity for each age class of pollock (latitude/longitude projected in NAD83), averaged over the survey period (1982–2019). [Colour online.]

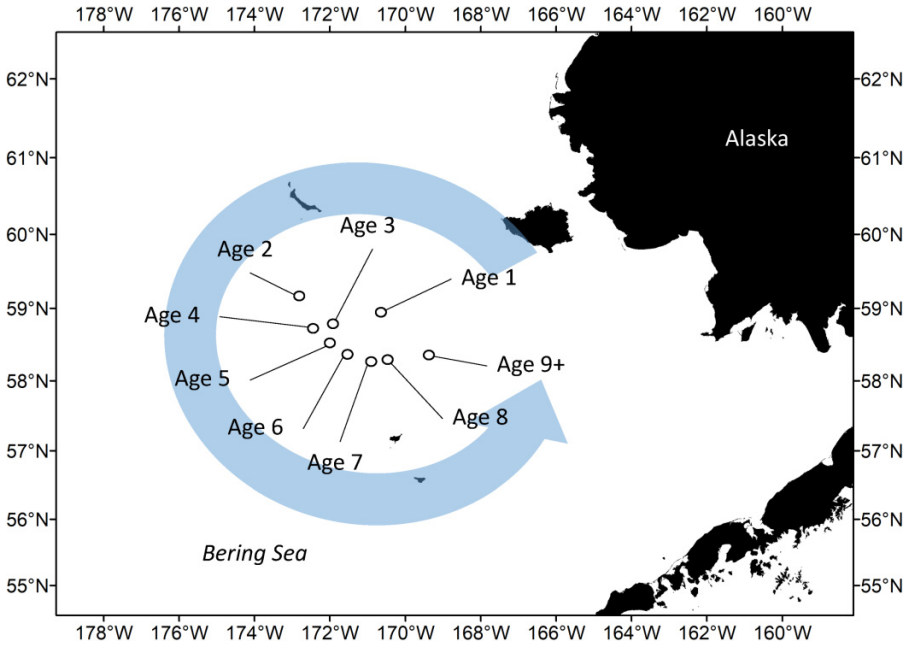

Fig. 3. Estimates of effective area occupied (±2 SE) for each age class of pollock, averaged over the survey period (1982–2019).

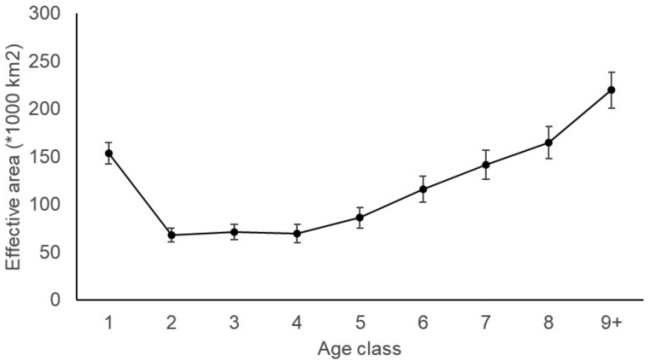

The effects of environmental factors on the EAO by pollock differed by age class. The effect of cold pool area was significant for age classes 1, 2, 7, 8, and 9+ (Fig. 6). In general, it appears that EAO declines with increasing cold pool area. The effect of the cold pool on EAO of age classes 3–6 was not significant and the partial effect was nearly constant, indicating that the cold pool likely does not affect EAO for these ages. For surface temperature (Fig. 7), the nonlinear interaction between surface temperature and EAO was significant for most adult pollock (age-5 through age-9+), and partial effect plots showed a similar pattern of increasing EAO with increasing surface temperatures for all significant age classes. This result indicates that pollock of these ages are more concentrated in smaller areas in cooler temperatures, and more dispersed in warmer conditions. However, this effect appears to be most pronounced only for surface temperatures larger than 7 °C, which indicates that this dispersion occurs only during warm summers.

Discussion

This analysis describes the spatial distribution of pollock in their summer feeding habitat as a function of ontogeny and size. We also provide the first evidence for a cohort effect in the spatial distribution of the pollock of the EBS, and show that intrinsic and extrinsic factors affect the spatial distribution of the population in age-specific ways.

The youngest and oldest classes of pollock are broadly dispersed across the continental shelf in the EBS, although they are rarely encountered in the southern portion of the survey range. In contrast, intermediate age classes are more concentrated in feeding areas near the shelf edge. Although ontogenetic migration has been widely demonstrated in marine fish species and has been previously examined in pollock (Bailey et al. 1999; Ianelli 2005) in the Bering Sea, previous studies have not accounted for spatial variability in age structure. In contrast, our study accounted for spatiotemporal variability in age–length relationships by using model-based age composition estimation. Ignoring this variability can lead to biased outcomes of assessment models (Correa et al. 2020) and in spatiotemporal analysis of ontogenetic migrations.

Our results suggest that the youngest and oldest age classes of pollock undertake more limited summer feeding migrations than intermediate age classes, as they appear to be less concentrated in summer feeding areas as demonstrated by EAO by age. Due to their size and limited swimming performance, age-1 pollock have limited ability to cover large distances, and their wide dispersal across the EBS shelf, and

Fig. 4. Temporal trends in centers of gravity by latitude (top) and longitude (center), as well as effective area occupied (bottom) for all age classes of pollock.

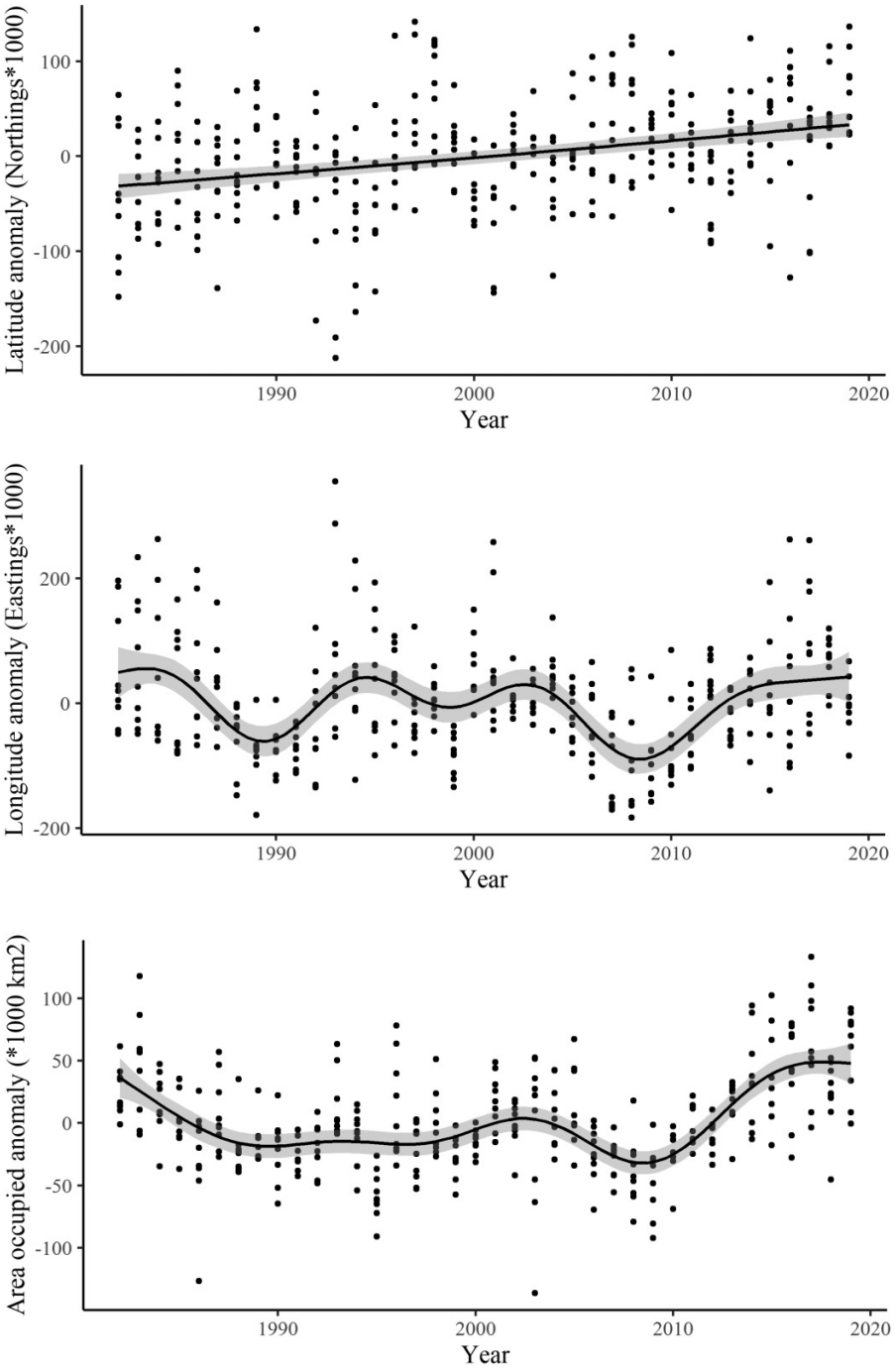

their absence from the southeastern portion of the Bering Sea survey area, is likely a reflection of the distribution of the larval and age-0 population distribution, which is driven by ocean currents. This advective extrinsic factor varies among years (Wespestad et al. 2000). Kotwicki et al. (2005) also found that smaller pollock (<29 cm, roughly corresponding to age-1 and age-2) do not aggregate along the shelf edge as much as older pollock. Larger juvenile and adult pollock can migrate over larger distances and form tighter, more pelagic aggregations. These aggregations form predominantly on the shelf edge, which is a primary pollock feeding ground (Kotwicki et al. 2005). As pollock mature, their summer distribution moves progressively to the south along the shelf edge. Eventually, older pollock disperse again over the shallow parts of the shelf. This dispersal coincides with the transition of pollock from predominantly pelagic prey to more diverse prey that consists of both pelagic and benthic animals (Buckley et al. 2016), limiting the requirement for an extensive feeding migration. Previous studies have also suggested that juvenile pollock move offshore and northward during the first

Table 1. *P* values relating pairwise comparisons of global index of colocation (GIC) within year (above diagonal) or within cohort (below diagonal) to pairwise comparisons among age classes for all years/cohorts.

	Age-1	Age-2	Age-3	Age-4	Age-5	Age-6	Age-7	Age-8	Age-9
Age-1	—	**0.04**	0.47	0.75	0.67	0.72	0.38	0.18	0.34
Age-2	0.07	—	**0.02**	0.05	0.07	0.16	0.23	0.33	0.44
Age-3	0.52	0.07	—	**<0.01**	0.05	0.30	0.32	0.47	0.58
Age-4	0.45	0.19	**<0.01**	—	**<0.01**	**<0.01**	0.08	0.40	0.61
Age-5	0.43	0.08	**<0.01**	**<0.01**	—	**<0.01**	**<0.01**	0.07	0.40
Age-6	0.63	0.15	**<0.01**	**<0.01**	**<0.01**	—	**<0.01**	**<0.01**	0.29
Age-7	0.26	0.20	0.09	**0.04**	**<0.01**	**<0.01**	—	**<0.01**	**0.02**
Age-8	0.26	0.07	0.31	0.37	0.10	**<0.01**	**<0.01**	—	**<0.01**
Age-9	0.49	0.51	0.74	0.83	0.70	0.55	0.10	0.18	—

Note: Significant *P* values (<0.05, in bold) suggest greater correlation among age classes within year/cohort.

Table 2. *P* values relating pairwise comparisons of Schoener's *D* within year (above diagonal) or within cohort (below diagonal) to pairwise comparisons among age classes for all years/cohorts.

	Age-1	Age-2	Age-3	Age-4	Age-5	Age-6	Age-7	Age-8	Age-9
Age-1	—	**<0.01**	**<0.01**	0.08	0.13	0.19	0.20	0.14	0.16
Age-2	0.13	—	**<0.01**	**<0.01**	**<0.01**	**<0.01**	**<0.01**	**<0.01**	0.07
Age-3	0.33	**<0.01**	—	**<0.01**	**<0.01**	**<0.01**	**<0.01**	**<0.01**	0.16
Age-4	0.28	0.05	**<0.01**	—	**<0.01**	**<0.01**	**<0.01**	**<0.01**	0.05
Age-5	0.15	0.10	**<0.01**	**<0.01**	—	**<0.01**	**<0.01**	**<0.01**	**<0.01**
Age-6	0.31	**0.01**	**0.02**	**<0.01**	**<0.01**	—	**<0.01**	**<0.01**	**<0.01**
Age-7	0.37	0.13	**<0.01**	**0.03**	**<0.01**	**<0.01**	—	**<0.01**	**<0.01**
Age-8	0.39	0.13	0.15	0.07	0.06	**<0.01**	**<0.01**	—	**<0.01**
Age-9	0.56	0.54	0.55	0.73	0.59	0.56	**0.01**	**<0.01**	—

Note: Significant *P* values (<0.05, in bold) suggest greater correlation among age classes within year/cohort.

Table 3. Summary of variance decomposition, in which age-specific centers of gravity (decomposed into latitude and longitude) are related to the factor variables: year and cohort.

	First	Last	Avg.
Latitude deviation ~ factor(Year) + factor(Cohort)			
Total variance explained: 0.633			
Factor(Year)	0.420	0.377	0.399
Factor(Cohort)	0.256	0.213	0.235
Longitude deviation ~ factor(Year) + factor(Cohort)			
Total variance explained: 0.610			
Factor(Year)	0.443	0.363	0.403
Factor(Cohort)	0.247	0.168	0.208

Note: First: variance explained by each predictor alone; last: variance explained when the predictor is added to the model as second.

few years of life, then generally move southward and back onto the shelf after age-3 (Bailey et al. 1999; Ianelli 2005).

In addition to ontogenetic migration, our data show evidence of a recent northward shift of the overall pollock COG in the Bering Sea, particularly during 2016–2019 for most age classes. In recent years, this northward shift in distribution was accompanied by an increase in EAO, which indicates that the recent expansion to the north does not coincide with corresponding reductions of the area occupied in the south. If the warming trend continues in the Bering Sea, we can expect further expansion of pollock distribution to the north (as demonstrated in recent pollock studies in the northern Bering Sea; Stevenson and Lauth 2019). This may hamper the ability of the EBS bottom trawl survey to assess year-class strength and recruitment success, as was the case for the 1992 year class, much of which was advected outside the survey area (Wespestad et al. 2000; O'Leary et al. 2020). If further expansions to the north continue and the southern extent of pollock distribution remains unchanged, we may see a further increase in the EAO of the pollock population in the Bering Sea in the future. Such increases in summer EAO can negatively affect the commercial fisheries because fish are more dispersed, and fishing quotas require more time and effort to fill. This situation was observed in 2018–2020 in the EBS pollock summer fishing season, when it took longer than usual to catch the quota (Ianelli et al. 2021). The effect of the expansion of the summer EAO on the population size and structure is unclear and requires further investigation.

Our comparisons of spatial correlation among years and cohorts provide evidence of a population-level "cohort effect". This effect is also clear from our decomposition of variance in the COG among years and cohorts. Marquez et al. (2021) showed a cohort effect in the spatial autocorrelation in

Table 4. Summary of variable selection process for the GAM modeling effective area occupied.

	Variable									
		Cold pool area								
Model	btemp	Area <2 °C	Area <1 °C	Area <0 °C	stemp	ssb	rec	age	% Var. explained	AIC
Model_1	*s*	—	—	—	*s*	*s*	*s*	*f*	75.9	8115.1
Model_2	—	*s*	—	—	*s*	*s*	*s*	*f*	75.0	8125.3
Model_3	—	—	*s*	—	*s*	*s*	*s*	*f*	75.2	8122.2
Model_4	—	—	—	*s*	*s*	*s*	*s*	*f*	76.0	8110.5
Model_4.1	—	—	—	by=age	*s*	*s*	*s*	*f*	78.1	8102.7
Model_4.2	—	—	—	*s*	by=age	*s*	*s*	*f*	78.1	8101.7
Model_4.3	—	—	—	*s*	*s*	by=age	*s*	*f*	77.5	8108.3
Model_4.4	—	—	—	*s*	*s*	*s*	by=age	*f*	74.9	8140.2
Model_4.2.1∗	—	—	—	by=age	by=age	*s*	*s*	*f*	80.6	8092.9
Model_4.2.2	—	—	—	*s*	by=age	by=age	*s*	*f*	79.2	8104.5
Model_4.2.3	—	—	—	*s*	by=age	*s*	by=age	*f*	77.2	8136.3
Model_4.2.1.1	—	—	—	by=age	by=age	by=age	*s*	*f*	80.9	8104.2
Model_4.2.1.2	—	—	—	by=age	by=age	*s*	by=age	*f*	79.6	8125.2

Notes:*s*: variable modeled as a smooth term; *f*: variable modeled as a factor; "by=age": variable modeled as a factor–smooth interaction with "age" as the factor. Asterisk (∗) indicates the final preferred model, using AIC as the optimality criterion (in which a lower value indicates a more optimized model).

density for cod and haddock in the Barents Sea, and noted that this effect was increasingly prevalent in older age classes in both species. Our results show an analogous cohort effect in the temporal autocorrelation among age classes of pollock in the Bering Sea, though we do not see clear evidence that this effect is more prevalent among older age classes. The magnitude of the cohort effect demonstrated here is about half of the year effect, so clearly it should not be omitted from studies of spatial dynamics in EBS pollock. Because our variance decomposition analysis has compartmentalized spatial correlation into interannual effects and cohort effects, and generalized across a large number of survey years, spatial variance explained by the cohort effect should be due primarily to the initial distribution of the cohort. This, in turn, should reflect the relative spawning success of the component spawning aggregations that comprise the Bering Sea pollock population. The fact that we show here a clear cohort effect implies that spawning success can differ among different spawning aggregations, and that these differences in spawning success may lead to persistent differences in the spatial distributions of cohorts as they recruit to the adult population.

The presence of a persistent cohort effect may indicate that there is some level of metapopulation structure in the pollock of the Bering Sea. If this is the case, then mechanisms must exist to maintain the structure in a region without clearly defined geographic boundaries. These mechanisms could include physical oceanographic patterns, genetic predisposition and environmental imprinting, or entrainment by learning adult migratory patterns. Spawning aggregations of pollock in the EBS are broadly distributed in time and space (Hinckley 1987; Stahl and Kruse 2008). Their eggs and larvae are subject to variable physical transport (Wespestad et al. 2000) and mixing, resulting in multiple size-modes of larvae that overlap in geographic distribution across the EBS (Nishimura et al. 1996; Traynor and Smith 1996). Thus, larval retention in natal regions by physical oceanographic isolating mechanisms appears unlikely. If a genetic and (or) imprinted predisposition exists for spawning within a particular area and time, then pollock would have a greater chance of spawning within aggregations of similarly predisposed pollock than with others. Alternatively, juvenile pollock may learn migration patterns by following adults to spawning locations, a process known as entrainment (Petitgas et al. 2006), which could explain the increased area occupied when spawning biomass is large (MacCall et al. 2019). Our study cannot distinguish between these and other specific behavioral mechanisms that may result in the spatiotemporal patterns identified here. However, the presence of a persistent cohort effect in the spatial distribution of the population suggests that this phenomenon requires more study, as the relative influences of structuring mechanisms (genetic/environmental imprinting vs. behavioral entrainment) may have important implications for the ability of the species to colonize new habitat or recolonize historic spawning habitat.

Extrinsic environmental factors are clearly important in determining the spatial distribution of pollock. For example, our most effective measure of temperature conditions near the sea floor, the cold pool area (<0° C), has an inverse relationship with the EAO by pollock on the Bering Sea shelf. In general, the more of the shelf is covered by the cold pool, the less of the shelf pollock occupy. This effect is also evident in the relationship of EAO to surface temperature, with pollock occupying more area on the shelf during years of warmer overall surface temperatures. In general,

Table 5. Results of the final GAM modeling effective area occupied.

Formula: EAO ~ factor(age) + *s*(cpa, by=factor(age)) + *s*(stemp, by=factor(age)) + *s*(ssb) + *s*(rec)				
Parametric coefficients				
	Estimate	SE	*t* value	Pr(>|*t*|)
(Intercept)	154 809	4882	31.709	<0.001
factor(age)2	−85 700	7257	−11.810	<0.001
factor(age)3	−81 488	7284	−11.188	<0.001
factor(age)4	−82 387	7343	−11.219	<0.001
factor(age)5	−65 860	6156	−9.203	<0.001
factor(age)6	−37 806	6920	−5.463	<0.001
factor(age)7	−10 951	6811	−1.608	0.1089
factor(age)8	12 608	6758	1.866	0.0631
factor(age)9	69 638	6709	10.380	<0.001
Approximate significance of smooth terms				
	Edf	Ref.df	*F*	*P* value
s(cpa):factor(age)1	1.736	2.103	3.801	0.022
s(cpa):factor(age)2	1.000	1.000	7.442	0.006
s(cpa):factor(age)3	1.000	1.000	1.474	0.226
s(cpa):factor(age)4	1.000	1.000	0.089	0.765
s(cpa):factor(age)5	1.000	1.000	0.000	0.990
s(cpa):factor(age)6	1.000	1.000	0.367	0.545
s(cpa):factor(age)7	2.731	2.938	3.267	0.032
s(cpa):factor(age)8	2.880	2.984	7.111	<0.001
s(cpa):factor(age)9	2.939	2.997	9.564	<0.001
s(stemp):factor(age)1	2.173	2.572	0.270	0.667
s(stemp):factor(age)2	1.000	1.000	1.539	0.216
s(stemp):factor(age)3	1.581	1.939	1.051	0.399
s(stemp):factor(age)4	1.526	1.867	2.749	0.127
s(stemp):factor(age)5	2.393	2.759	3.295	0.015
s(stemp):factor(age)6	2.283	2.675	4.592	0.003
s(stemp):factor(age)7	1.986	2.410	2.776	0.035
s(stemp):factor(age)8	1.989	2.417	4.487	0.005
s(stemp):factor(age)9	1.000	1.000	4.234	0.040
s(ssb)	2.849	2.977	3.355	0.021
s(rec)	2.964	2.998	9.879	<0.001

this makes sense, as several previous studies have concluded that adult pollock avoid low temperatures (Wyllie-Echeverria 1995; Wyllie-Echeverria and Wooster 1998; Kotwicki 2005; Kotwicki and Lauth 2013), particularly <0 °C. Some authors have suggested that juvenile pollock may use the cold pool as a refuge from predatory pressures, including cannibalism by larger pollock (Hunsicker et al. 2013; Uchiyama et al. 2020). However, whether this avoidance is the result of a direct physiological response or an indirect response to ecological parameters such as prey populations or predator avoidance is still unclear.

Our results also suggest that interannual temperature variations do not affect the spatial distribution of all ages of pollock in the same way. The effect of bottom temperature was significant for the youngest and oldest age classes of pollock, but not intermediate age classes. In contrast, the effect of surface temperature was significant only for adults. These age-specific differences in the response of pollock populations to temperature could be due to several factors. Young pollock recruits are unable to escape colder temperatures (Buckley et al. 2016), but once swimming speed allows active schooling and cross-shelf migration, behavioral adaptations to maximize average feeding and survival success drive the distributions (Kotwicki et al. 2005). At larger sizes, pollock become less susceptible to predation, less dependent on small pelagic prey (Buckley et al. 2016), more benthic in habit (Lynde 1984; Bakkala and Alton 1986; Traynor et al. 1990), and disperse more widely over the EBS shelf during summer feeding migrations (Kotwicki et al. 2005). Additionally, there is evidence that the influence of temperature on bioenergetic parameters, such as respiration and digestion, declines with increasing size in pollock (Buckley and Livingston 1994), so larger pollock may be less metabolically dependent on optimum temperatures. Finally, the fact that bottom and surface

Fig. 5. Partial effect plots from selected GAM model showing relationships between (A) age class and effective area occupied (EAO); (B) standing stock biomass and EAO; and (C) age-1 abundance and EAO for pollock in the eastern Bering Sea.

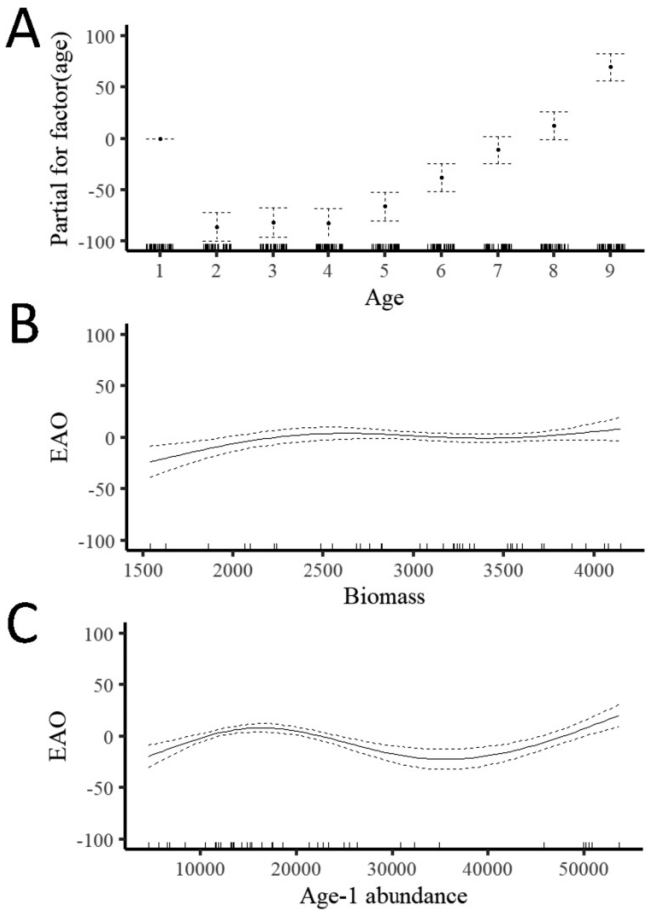

temperature have different relationships to pollock distribution may be due to the differing seasonal dynamics of these environmental parameters. Surface temperature changes steadily over the summer as the surface waters warm due to increased seasonal solar heating, while bottom temperature, and particularly cold pool area, is driven more by the ice conditions of the previous winter and often persists through much or all of the summer (Stabeno et al. 2007).

In addition to extrinsic factors, intrinsic population factors affect the spatial distribution of pollock, though not to the same extent. If density-dependent factors influence the spatial distribution of pollock, then we would expect to see a strong relationship between standing stock biomass (the overall size of the population) and the geographic area occupied by the population. Our results do not show clear evidence of this effect at higher population levels, but there is some indication that the area occupied by the population does contract when the overall biomass is particularly low. Of course, pollock may expand their range into neighboring regions at high abundance levels (e.g., Tsugi 1989; Stepanenko 1997), so at times the population is likely expanding outside the survey area, into the northern Bering Sea, south into the Gulf of Alaska, or west past the US–Russia convention line (O'Leary et al. 2021). If new recruits drive the spatial distribution of the population, we would expect to see a strong relationship between age-1 abundance and area occupied, assuming that the proportion of the population in the survey area remains constant. Again, our results do not show clear evidence of this effect except for the few largest cohorts in the time series, and adding an age interaction to the recruitment term in the model degraded the fit. In fact, age-1 abundance was not significantly related to the area occupied by the age-1 segment of the population. This suggests that either age-1 abundance is not reaching sufficient levels for density to become limiting, or that more of the population moves outside the survey area at higher abundance levels.

Although this study provides insight into the factors influencing the spatial distribution of pollock in the Bering Sea, the analysis has some important limitations. First, the availability of pollock to the survey trawl may be partially size-dependent. If age groups migrate differently within the survey area, as this study and Kotwicki et al. (2005) suggest, then it is also possible that the proportions of the population within the survey area, and therefore available to the trawl survey, are not consistent among population segments and survey years. Additionally, the vertical distribution of pollock in the water column largely influences their availability to the bottom trawl gear. This vertical distribution may differ substantially among different age classes of pollock, and the proportion of the population near the bottom varies both spatially and over time (Monnahan et al. 2021). This study only examined the distribution of pollock available to the bottom trawl survey, and subadult pollock in the 20–40 cm size range are less commonly encountered on AFSC bottom trawl surveys (Lauth et al. 2019). Therefore, estimates of the spatial distribution for these age classes may be more uncertain than those of the other age classes. We recommend additional research conducting similar analyses using a joint model of bottom trawl and acoustic data to assess the pelagic portion of the population as well.

Secondly, our analyses do not address the possibility of time-lagged effects of intrinsic and extrinsic factors. For example, the cold pool area in the survey year 2002 may have affected the spatial distribution of the pollock population in 2003. Finally, the precision of density-at-age estimation declines with species age class. Although our method of estimating age compositions accounts for spatial differences in growth rates, the fact remains that the age–length key assigns larger pollock to an age class with less precision. This lack of precision may affect on the power of our analyses to detect factors of influence for the older age classes.

Overall, the results of this study indicate that interannual variability in the spatial distribution of the pollock population in the EBS is strongly influenced by extrinsic environmental factors, but that the population distribution also has a cohort component that explains nearly one-third of the variance in COG. Furthermore, this study shows that intrinsic and extrinsic factors affect different age groups of the population in different ways. Thus, when assessing the spatiotemporal distribution dynamics of marine fish populations, it is essential not only to model intrinsic factors, extrinsic factors,

Fig. 6. Partial effect plots from selected GAM model showing relationships between the estimated area of the cold pool (km^2 less than 0 °C) and effective area occupied (EAO) for all ages of pollock in the eastern Bering Sea.

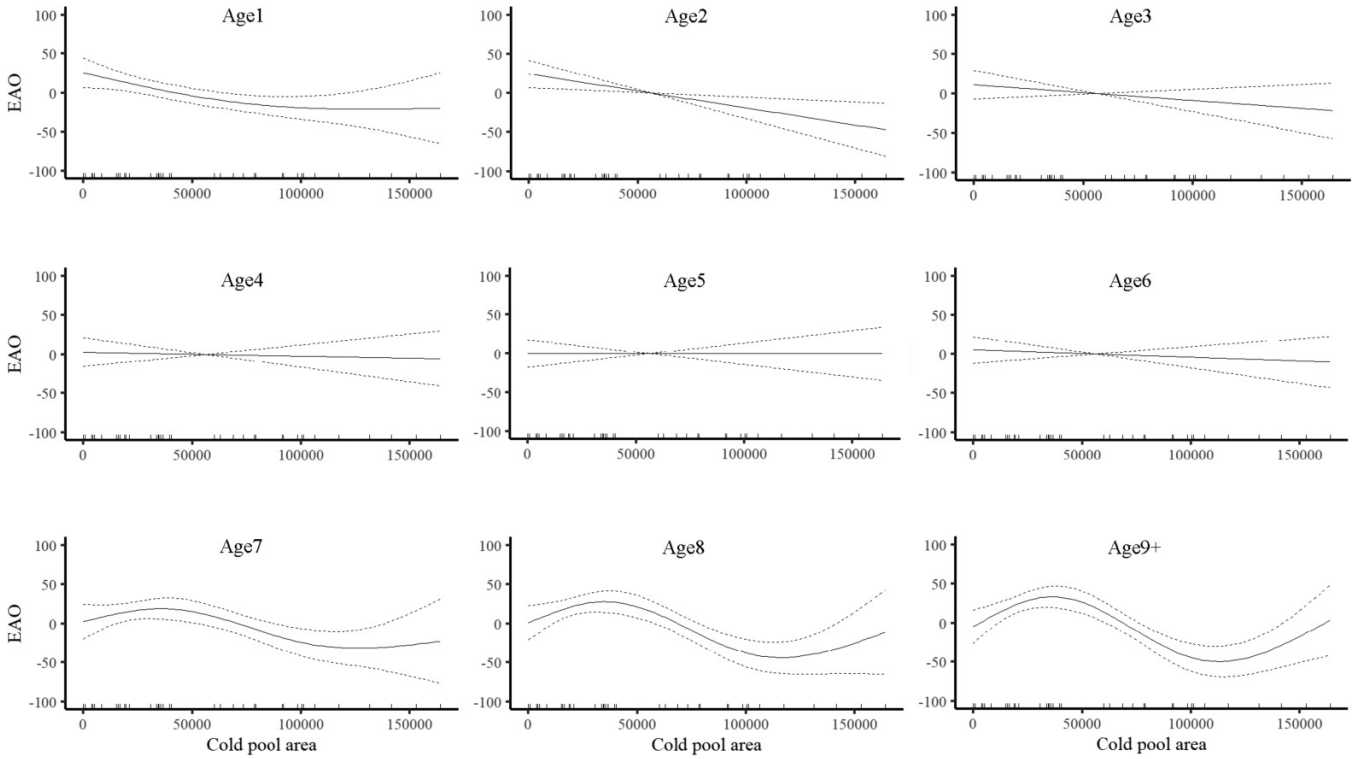

Fig. 7. Partial effect plots from selected GAM model showing relationships between the mean annual surface temperature and effective area occupied (EAO) for all ages of pollock in the eastern Bering Sea.

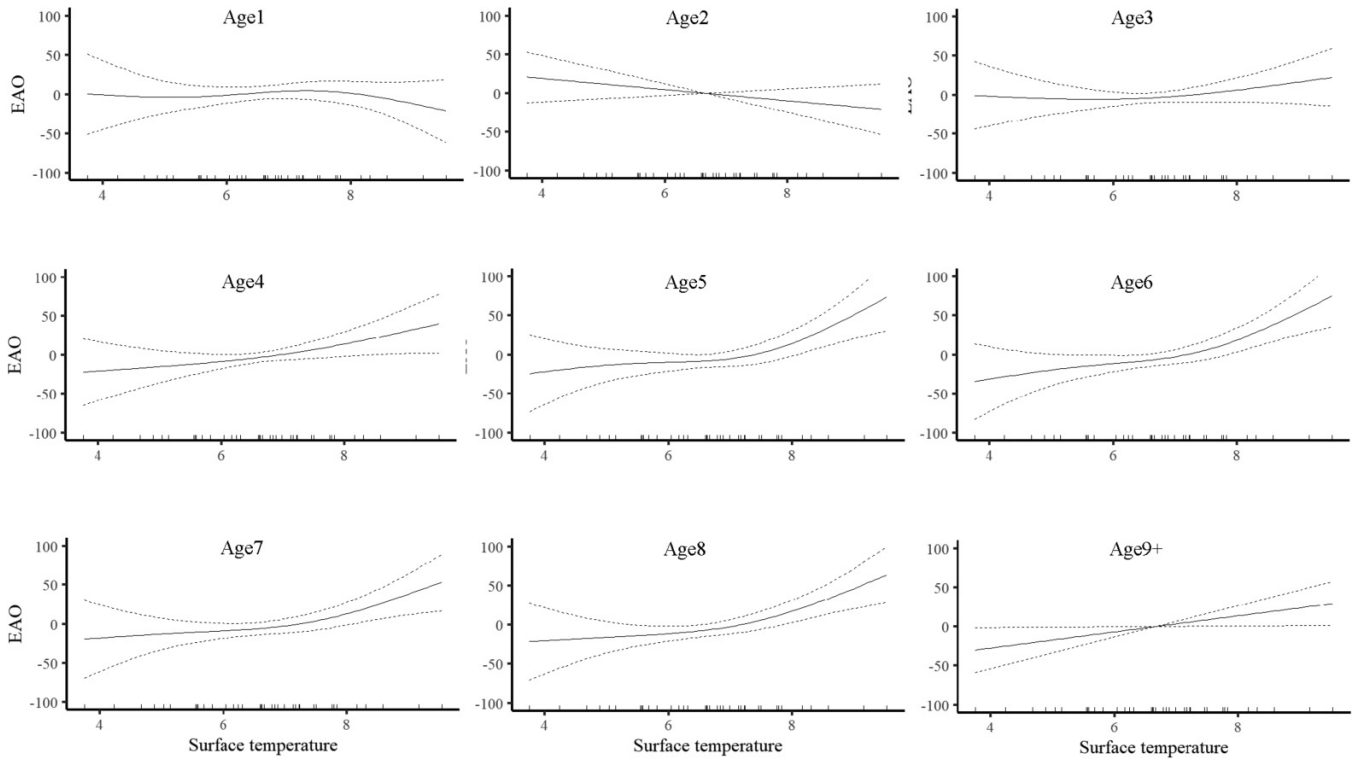

and spatial cohort components, but also to consider variability in how these factors influence the distribution of different age classes in the population.

Acknowledgements

We thank C. O'Leary and J. Ianelli (AFSC) for reviewing an earlier version of this manuscript. We also thank the multitude of scientists in the AFSC's Groundfish Assessment Program, and the fishing crews on the numerous chartered vessels, who have worked to produce this remarkable database over the past 40 years.

Article information

History dates

Received: 4 November 2021
Accepted: 14 June 2022
Accepted manuscript online: 27 June 2022
Version of record online: 4 October 2022

Data availability

Primary data used in this study can be located on the Alaska Fisheries Information Network (https://akfin.psmfc.org/). Primary catch data for GAP bottom-trawl surveys can be located at the NOAA Fisheries One Stop Shop (www.fisheries.noaa.gov/foss).

Author information

Author ORCIDs

Duane E. Stevenson https://orcid.org/0000-0003-0967-8400
Stan Kotwicki https://orcid.org/0000-0002-6112-5021
James T. Thorson https://orcid.org/0000-0001-7415-1010

Competing interests

The authors declare that they have no known competing financial interests or personal relationships that could have appeared to influence the work reported in this paper.

Supplementary material

Supplementary data are available with the article at https://doi.org/10.1139/cjfas-2021-0300.

References

Bacheler, N.M., Ciannelli, L., Bailey, K.M., and Duffy-Anderson, J.T. 2010. Spatial and temporal patterns of walleye pollock (*Theragra chalcogramma*) spawning in the eastern Bering Sea inferred from egg and larval distributions. Fish. Oceanogr. **19**: 107–120. doi:10.1111/j.1365-2419.2009.00531.x.

Bailey, K.M., Quinn, T.J., Bentzen, P., and Grant, W.S. 1999. Population structure and dynamics of walleye pollock *T heragra chalcogramma*. Adv. Mar. Biol. **37**: 179–255. doi:10.1016/S0065-2881(08)60429-0.

Bakkala, R.G., and Alton, M.S. 1986. Evaluation of demersal trawl survey data for assessing the condition of eastern Bering Sea pollock. Int. N. Pac. Fish. Comm. Bull. **45**: 90–120.

Benoit-Bird, K.J., McIntosh, N.E., and Heppell, S.A. 2013. Nested scales of spatial heterogeneity in juvenile walleye pollock *T heragra chalcogramma* in the southeastern Bering Sea. Mar. Ecol. Prog. Ser. **484**: 219–238. doi:10.3354/meps10319.

Berg, C.W., and Kristensen, K. 2012. Spatial age–length key modelling using continuation ratio logits. Fish. Res. **129–130**: 119–126. doi:10.1016/j.fishres.2012.06.016.

Bez, N., and Rivoirard, J. 2000. Indices of collocation between populations. *In* Workshop on the use of continuous underway fish egg sampler (CUFES) for mapping spawning habitat of pelagic fish. *Edited by* D.M. Checkley, J.R. Hunter, L. Motos and C.D. von der Lingen. GLOBEC Report. pp. 48–52.

Buckley, T.W., and Livingston, P.A. 1994. A bioenergetics model of walleye pollock (*Theragra chalcogramma*) in the eastern Bering Sea: structure and documentation. U.S. Dep. Commer., NOAA Tech. Memo. NMFS-AFSC-37, 55pp.

Buckley, T.W., Ortiz, I., Kotwicki, S., and Aydin, K. 2016. Summer diet composition of walleye pollock and predator-prey relationships with copepods and euphausiids in the eastern Bering Sea, 1987–2011. Deep-Sea Res. II, **134**: 302–311. doi:10.1016/j.dsr2.2015.10.009.

Burnham, K.P., and Anderson, D.R. 2002. Model selection and multimodel inference: a practical information-theoretic approach. Springer-Verlag, New York, 488pp.

Christensen, R. 1992. Comment on Chevan and Sutherland. Am. Stat. **46**: 74.

Correa, G.M., Ciannelli, L., Barnett, L.A.K., Kotwicki, S., and Fuentes, C. 2020. Improved estimation of age composition by accounting for spatiotemporal variability in somatic growth. Can. J. Fish. Aquat. Sci. **77**(11): 1810–1821. doi: 10.1139/cjfas-2020-0166. PMID: 32461710.

Duffy-Anderson, J.T., Ciannelli, L., Honkalehto, T., Bailey, K.M., Sogard, S.M., Springer, A.M., and Buckley, T. 2003. Distribution of age-1 and age-2 walleye pollock in the Gulf of Alaska and eastern Bering Sea: sources of variation and implications for higher trophic levels. *In* The big fish bang. Proceedings of the 26th annual larval fish conference. *Edited by* H.I. Browman and A.B. Skiftesvik. Institute of Marine Research, Bergen, Norway. pp. 381–394.

Duffy-Anderson, J.T., Stabeno, P.J., Siddon, E.C., Andrews, A.G., Cooper, D.W. Eisner, L.B., et al. 2017. Return of warm conditions in the southeastern Bering Sea: phytoplankton – fish. PLoS ONE, **12**(6): e0178955. doi:10.1371/journal.pone.0178955. PMID: 28658253.

Eisner, L.S., Zuenko, Y.I., Basyuk, E.O., Britt, L.L., Duffy-Anderson, J.T. Kotwicki, S., et al. 2021. Environmental impacts on walleye pollock (*Gadus chalcogrammus*) distribution across the Bering Sea shelf. Deep Sea Res. II: Top. Stud. Oceanogr. **181–182**: 104881. doi:10.1016/j.dsr2.2020.104881.

Fredston-Hermann, A., Selden, R., Pinsky, M., Gaines, S.D., and Halpern, B.S. 2020. Cold range edges of marine fishes track climate change better than warm edges. Glob. Change Biol. **26**: 2908–2922. doi:10.1111/gcb.15035.

Grömping, U. 2006. Relative importance for linear regression in R: the package relaimpo. J. Stat. Soft. **17**: 1–27. doi:10.18637/jss.v017.i01.

Hinckley, S. 1987. The reproductive biology of walleye pollock, *T heragra chalcogramma*, in the Bering Sea, with reference to spawning stock structure. Fish. Bull. **85**: 481–498.

Hoff, G.R. 2010. Identification of skate nursery habitat in the eastern Bering Sea. Mar. Ecol. Prog. Ser. **403**: 243–254. doi:10.3354/meps08424.

Honkalehto, T., McCarthy, A., Ressler, P., Stienessen, S., and Jones, D. 2010. Results of the acoustic-trawl survey of walleye pollock (*Theragra chalcogramma*) on the U.S. and Russian Bering Sea shelf in June–August 2009 (DY0909). AFSC Processed Rep. 2010-03, Alaska Fish. Sci. Cent., NOAA, Natl. Mar. Fish. Serv., Seattle,WA. 57 pp.

Hunsicker, M.E., Ciannelli, L., Bailey, K.M., Zador, S., and Stige, L.C. 2013. Climate and demography dictate the strength of predator–prey overlap in a subarctic marine ecosystem. PLoS ONE, **8**: e66025. doi:10.1371/journal.pone.0066025. PMID: 23824707.

Hutchinson, G.E. 1957. Concluding remarks. Cold Spring Harbor Symposia on Quantitative Biology, Vol 22. pp.415–427. doi:10.1101/SQB.1957.022.01.039.

Ianelli, J. 2005. Assessment and fisheries management of eastern Bering Sea walleye pollock: is sustainability luck? Bull. Mar. Sci. **76**: 321–335.

Ianelli, J., Fissel, B., Holsman, K., Honkalehto, T., Kotwicki, S. Monnahan, C., et al. 2019. Assessment of the walleye pollock stock in the eastern Bering Sea. *In* Stock assessment and fishery evaluation report for the groundfish resources of the Bering Sea/Aleutian Islands regions. Plan Team for the Groundfish Fisheries of the Bering Sea and Aleutian Islands. Chapter 1, 169 pp.

Ianelli, J., Fissel, B., Stienessen, S., Honkalehto, T., Siddon, E., and Allen-Akselrud, C. 2021. Chapter 1: Assessment of the walleye pollock stock in the eastern Bering Sea. In 2021 Stock assessment and fishery evaluation report for the groundfish resources of the Bering Sea and Aleutian Islands regions. North Pacific Fishery Management Council. pp. 48–52.

Kastelle, C.R., and Kimura, D.K. 2006. Age validation of walleye pollock (*Theragra chalcogramma*) from the Gulf of Alaska using the disequilibrium of Pb-210 and Ra-226. ICES J. Mar. Sci. **63**: 1520–1529. doi:10.1016/j.icesjms.2006.06.002.

Kim, S., Kendall, A.W., Jr., and Kang, S. 1996. The abundance and distribution of pollock eggs and some spawning characteristics in the southeastern Bering Sea in 1977. Ocean Res. **18**(Special): 59–67.

Kotwicki, S., and Lauth, R.R. 2013. Detecting temporal trends and environmentally-driven changes in the spatial distribution of bottom fishes and crabs on the eastern Bering Sea shelf. Deep-Sea Res. **94**: 231–243.

Kotwicki, S., Buckley, T.W., Honkalehto, T., and Walters, G. 2005. Variation in the distribution of walleye pollock (*Theragra chalcogramma*) with temperature and implications for seasonal migration. Fish. Bull. **103**: 574–587.

Kotwicki, S., Horne, J.K., Punt, A.E., and Ianelli, J.N. 2015. Factors affecting the availability of walleye pollock to acoustic and bottom trawl survey gear. ICES J. Mar. Sci. **72**: 1425–1439. doi:10.1093/icesjms/fsv011.

Kristensen, K., Nielsen, A., Berg, C.W., Skaug, H., and Bell, B.M. 2016. TMB: automatic differentiation and Laplace approximation. J. Stat. Soft. **70**: 1–21. doi:10.18637/jss.v070.i05.

Laman, E.A., Rooper, C.N., Turner, K., Rooney, S., Cooper, D.W., and Zimmermann, M. 2018. Using species distribution models to describe essential fish habitat in Alaska. Can. J. Fish. Aquat. Sci. **75**: 1230–1255. doi:10.1139/cjfas-2017-0181.

Lauth, R.R., Dawson, E.J., and Conner, J. 2019. Results of the 2017 eastern and northern Bering Sea continental shelf bottom trawl survey of groundfish and invertebrate fauna. U.S. Dep. Commer., NOAA Tech. Memo. NMFS-AFSC-396. 260pp.

Lindgren, F., Rue, H., and Lindström, J. 2011. An explicit link between Gaussian fields and Gaussian Markov random fields: the stochastic partial differential equation approach. J. Roy. Stat. Soc. Ser. B Stat. Methodol. **73**: 423–498. doi:10.1111/j.1467-9868.2011.00777.x.

Lynde, C.M. 1984. Juvenile and adult walleye pollock of the eastern Bering Sea: literature review and results of ecosystem workshop. *In* Proceedings of the workshop on walleye pollock and its ecosystem in the eastern Bering Sea. *Edited by* D.H. Ito. U.S. Dep. Commer., NOAA Tech. Memo. NMFS-F/NWC-62. 292pp.

MacCall, A.D., Francis, T.B., Punt, A.E., Siple, M.C., Armitage, D.R. Cleary, J.S., et al. 2019. A heuristic model of socially learned migration behavior exhibits distinctive spatial and reproductive dynamics. ICES J. Mar. Sci. **76**: 598–608. doi:10.1093/icesjms/fsy091.

Marquez, J.F., Saether, B.-E., Aanes, S., Engen, S., Salthaug, A., and Lee, A.M. 2021. Age-dependent patterns of spatial autocorrelation in fish populations. Ecology, **102**(12): e03523. doi:10.1002/ecy.3523.

Monnahan, C.C., Thorson, J.T., Kotwicki, S., Lauffenberger, N., Ianelli, J.N., and Punt, A.E. 2021. Incorporating vertical distribution in index standardization accounts for spatiotemporal availability to acoustic and bottom trawl gear for semi-pelagic species. ICES J. Mar. Sci. **78**(5): 1826–1839. doi: 10.1093/icesjms/fsab085. PMID: 33814897.

Nishimura, A., Mito, K., and Yanagimoto, T. 1996. Hatch date and growth estimation of juvenile walleye pollock, *T heragra chalcogramma*, collected in the Bering Sea in 1989 and 1990. *In* Ecology of juvenile walleye pollock, *Theragra chalcogramma*. *Edited by* R.D. Brodeur, P.A. Livingston, T.R. Loughlin and A.B. Hollowed. NOAA Tech. Rep. NMFS 126. pp. 81–87.

O'Leary, C.A., Thorson, J.T., Ianelli, J.N., and Kotwicki, S. 2020. Adapting to climate-driven distribution shifts using model-based indices and age composition from multiple surveys in the walleye pollock (*Gadus chalcogrammus*) stock assessment. Fish. Oceanogr. **29**: 541–557. doi:10.1111/fog.12494.

O'Leary, C.A., Kotwicki, S., Hoff, G.R., Thorson, J.T., Kulik, V.V. Ianelli, J.N., et al. 2021. Estimating spatiotemporal availability of transboundary fishes to fishery-independent surveys. J. App. Ecol. **58**(10): 2146–2157. doi: 10.1111/1365-2664.13914.

Parker-Stetter, S.L., Horne, J.K., and Urmy, S.S. 2015. Vertical distribution of age-0 walleye pollock during late summer: environment or ontogeny? Mar. Coast. Fish. **7**: 349–369. doi:10.1080/19425120.2015.1057307.

Petitgas, P., Reid, D., Planque, B., Nogueira, E., O'Hea, B., and Cotano, U. 2006. The entrainment hypothesis: an explanation for the persistence and innovation in spawning migration and life cycle patterns. ICES CM documents 2006/B:07.

Pinsky, M., Worm, B., Fogarty, M.J., Sarmiento, J.L., and Levin, S.A. 2013. Marine taxa track local climate velocities. Science, **341**: 1239–1242. doi:10.1126/science.1239352. PMID: 24031017.

Planque, B., Loots, C., Petitgas, P., Lindstrom, U., and Vaz, S. 2011. Understanding what controls the spatial distribution of fish populations using a multi-model approach. Fish. Ocean. **20**: 1–17. doi:10.1111/j.1365-2419.2010.00546.x.

R Core Team. 2020. R: a language and environment for statistical computing. R Foundation for Statistical Computing, Vienna, Austria. Available from https://www.R-project.org/.

Schoener, T.W. 1968. The *A nolis* lizards of Bimini: resource partitioning in a complex fauna. Ecology, **49**: 704–726. doi:10.2307/1935534.

Simpson, S.C., Eagleton, M.P., Olson, J.V., Harrington, G.A., and Kelly, S.R. 2017. Final essential fish habitat (EFH) 5-year review, summary report: 2010 through 2015. U.S. Dep. Commer., NOAA Tech. Memo. NMFS-F/AKR-15. 115p.

Smart, T.I., Siddon, E.C., and Duffy-Anderson, J.T. 2013. Vertical distributions of early life stages of walleye pollock (*Theragra chalcogramma*). Deep Sea Res. Part II: Top. Stud. Oceanogr. **94**: 201–210. doi:10.1016/j.dsr2.2013.03.030.

Stabeno, P.J., Bond, N.A., and Salo, S.A. 2007. On the recent warming of the southeastern Bering Sea shelf. Deep Sea Res. II: Top. Stud. Ocean. **54**: 2599–2618. doi:10.1016/j.dsr2.2007.08.023.

Stabeno, P.J., Duffy-Anderson, J.T., Eisner, L., Farley, E., Heintz, R., and Mordy, C.W. 2017. Return of warm conditions in the southeastern Bering Sea: physics to fluorescence. PLoS ONE, **12**: e0185464. doi:10.1371/journal.pone.0185464. PMID: 28957386.

Stahl, J.P., and Kruse, G.H. 2008. Spatial and temporal variability in size of maturity of walleye pollock in the eastern Bering Sea. Trans. Am. Fish. Soc. **137**: 1543–1557. doi:10.1577/T07-099.1.

Stepanenko, M.A. 1997. Variations from year to year in the spatial differentiation of the walleye pollock, *T heragra chalcogramma*, and the cod, *G adus macrocephalus*, in the Bering Sea. J. Ichthyol. **37**: 14–20.

Stevenson, D.E., and Lauth, R.R. 2019. Bottom trawl surveys in the northern Bering Sea indicate recent shifts in the distribution of marine species. Polar Biol. **42**: 407–421. doi:10.1007/s00300-018-2431-1.

Thorson, J.T. 2019. Guidance for decisions using the vector autoregressive spatio-temporal (VAST) package in stock, ecosystem, habitat and climate assessments. Fish. Res. **210**: 143–161. doi:10.1016/j.fishres.2018.10.013.

Thorson, J.T., and Barnett, L.A.K. 2017. Comparing estimates of abundance trends and distribution shifts using single- and multispecies models of fishes and biogenic habitat. ICES J. Mar. Sci. **74**: 1311–1321. doi:10.1093/icesjms/fsw193.

Thorson, J.T., and Minto, C. 2015. Mixed effects: a unifying framework for statistical modelling in fisheries biology. ICES J. Mar. Sci. **72**: 1245–1256. doi:10.1093/icesjms/fsu213.

Thorson, J.T., Pinsky, M.L., and Ward, E.J. 2016. Model-based inference for estimating shifts in species distribution, area occupied and centre of gravity. Methods Ecol. Evol. **7**: 990–1002. doi:10.1111/2041-210X.12567.

Thorson, J.T., Ianelli, J.N., and Kotwicki, S. 2017. The relative influence of temperature and size-structure on fish distribution shifts: a case-study on walleye pollock in the Bering Sea. Fish Fish. **18**: 1073–1084. doi:10.1111/faf.12225.

Thorson, J.T., Arimitsu, M.L., Barnett, L.A.K., Cheng, W., Eisner, L.B. Haynie, A.C., et al. 2021. Forecasting community reassembly using climate-linked spatio-temporal ecosystem models. Ecography, **44**: 1–14. doi:10.1111/ecog.05471.

Tierney, L., Kass, R.E., and Kadane, J.B. 1989. Fully exponential Laplace approximations to expectations and variances of nonpositive functions. J. Am. Stat. Assoc. **84**: 710–716. doi:10.1080/01621459.1989.10478824.

Traynor, J., and Smith, D. 1996. Summer distribution and abundance of age-0 walleye pollock, *T heragra chalcogramma*, in the Bering Sea. *In* Ecology of juvenile walleye pollock, *Theragra chalcogramma*. *Edited by* R.D. Brodeur, P.A. Livingston, T.R. Loughlin and A.B. Hollowed. NOAA Tech. Rep. NMFS 126. pp. 57–59.

Traynor, J.J., Karp, W.A., Sample, T.M., Furusawa, M., Sasaki, T. Teshima, K., et al. 1990. Methodology and biological results from surveys of walleye pollock (*Theragra chalcogramma*) in the eastern Bering Sea and Aleutian Basin in 1988. Int. N. Pac. Fish Comm. Bull. **50**: 69–99.

Tsugi, S. 1989. Alaska pollock population, *T heragra chalcogramma*, of Japan and its adjacent waters, I: Japanese fisheries and population studies. Mar. Freshw. Behav. Physiol. **15**: 147–205. doi:10.1080/10236248909378727.

Uchiyama, T., Mueter, F.J., and Kruse, G.H. 2020. Multispecies biomass dynamics models reveal effects of ocean temperature on predation of juvenile pollock in the eastern Bering Sea. Fish. Ocean. **29**: 10–22. doi:10.1111/fog.12433.

Wespestad, V.G., Fritz, L.W., Ingraham, W.J., and Megrey, B.A. 2000. On relationships between cannibalism, climate variability, physical transport and recruitment success of Bering Sea walleye pollock, *T heragra chalcogramma*. ICES J. Mar. Sci. **57**: 272–278. doi:10.1006/jmsc.2000.0640.

Woillez, M., Rivoirard, J., and Petitgas, P. 2009. Notes on survey-based spatial indicators for monitoring fish populations. Aquat. Living Res. **22**: 155–164. doi:10.1051/alr/2009017.

Wood, S. 2017. Generalized additive models: an introduction with R. 2nd ed. Chapman and Hall/CRC, London.

Wylllie-Echeverria, T. 1995. Sea-ice conditions and the distribution of walleye pollock (*Theragra chalcogramma*) on the Bering and Chukchi shelf. *In* Climate change and northern fish populations. Vol. 121. *Edited by* R.J. Beamish. Canadian Special Publication in Fisheries and Aquatic Science, National Research Council of Canada, Ottawa. pp. 131–136.

Wyllie-Echeverria, T., and Wooster, W.S. 1998. Year-to-year variations in Bering Sea ice cover and some consequences for fish distributions. Fish. Ocean. **7**: 159–170. doi:10.1046/j.1365-2419.1998.00058.x.

Zhang, J. 2016. R Package "spa". Available from https://www.rdocumentation.org/packages/spaa/versions/0.2.2.